

TDP-43 Knock Out and Neuronal Death in a Mouse Model of Frontotemporal Dementia

Written by Amanda Johnston

Completed under the direction of Dr. Yun Li

Background

1) Frontotemporal dementia (FTD)

Frontotemporal dementia (FTD) is a group of clinically and pathologically variable neurodegenerative diseases with a common selective loss of neurons in the frontal and temporal cortices that leads to progressive changes in behaviour, personality, and/or language with relative preservation of memory (Solomon). There presents an altered sociability and behavioural changes in anxiety and compulsivity alongside cognitive changes and motor symptoms, commonly associated with amyotrophic lateral sclerosis (ALS) (Neumann). FTD accounts for 5-15% of all dementias and is the second most common cause of dementias in the presenile age group (<65 years) after Alzheimer's Disease (AD) (Solomon).

Pathologically, postmortem brains of people who had FTD are characterized with a relatively selective frontotemporal lobar degeneration (FTLD), and like in most other neurodegenerative disorders, the presence of protein deposits forming distinct inclusion bodies in cells of the central nervous system (Solomon; Neumann). For a long period of time, the only well-characterized aggregation form in FTLD is the hyperphosphorylated tau protein, while a significant FTD cases were associated with tau-negative, ubiquitin-positive inclusions with unknown protein identity (Neumann). It wasn't until 2006 that TAR DNA-binding protein 43 (TDP-43) was identified as the major deposited component from the vast majority of FTD cases associated with tau-negative aggregations (Neumann). To most closely reflect the underlying pathogenic process, FTD cases can be categorized into several major molecular subgroups based on the disease-signifying protein deposits: FTLD-tau, FTLD-TDP, FTLD-FET and FTLD-UPs. Among these subgroups, the major deposited protein is TDP-43 in FTLD-TDP, ~50% of FTD cases, followed by tau (FTLD-tau, ~40% of FTD cases), and then Fused in sarcoma protein (FUS) (FTLD-FET, ~5%

of FTD cases) (Solomon). The remaining cases have ubiquitinated inclusions but do not contain any of the above proteins.

Degeneration consistently includes the frontal and temporal lobes while involvement of other cortical and subcortical structures such as the parietal cortex, basal ganglia, substantia nigra, and motor neurons is common although more variable among cases (Solomon). The amount and regional distribution of TDP-43 pathology in the central nervous system shows strong associations with the degree of neurodegeneration. However, despite the common feature of TDP-43 accumulation, significant heterogeneity is observed within FTLD-TDP cases with respect to morphology, inclusion types and distribution, and genetic associations (Balendra).

Genetically, around 1/3 of FTD cases have a known genetic cause, so called familial FTD (Solomon). 5-20% of familial FTD cases result from mutations in the progranulin gene (PGRN), a multifunctional secreted growth factor that regulates cell growth and survival, wound repair, and inflammation (Roberson). This mutation appears to cause disease and TDP-43 aggregation by reducing the amount of functional PGRN (haploinsufficiency) (Roberson). Despite the uniform molecular consequences of PGRN mutations, the clinical symptoms can vary significantly even among affected individuals within the same family, implicating additional genetic or environmental factors as disease modifiers (Roberson). The exact mechanism by which reduced levels of PGRN leads to neurodegeneration and TDP-43 aggregation is unknown; however, there is growing evidence for a role of lysosomal dysfunction as homozygous mutations in PGRN cause a form of lysosomal storage disease and FTD patients with PGRN haploinsufficiency show some histological and biochemical similarities with those cases (Roberson).

Another relevant mutation is the C9orf72 mutation wherein abnormal expansion of a GGGGCC hexanucleotide repeat in a noncoding region of the C9orf72 gene occurs (Balendra). This mutation is the

most common genetic cause of familial and sporadic forms of both FTD and ALS and the basis of most families in which both conditions occur (Balendra). For this mutation, three pathogenic mechanisms are proposed: 1) toxicity of proteins generated by unconventional repeat-associated non-ATG (RAN) translation of transcripts, 2) toxic RNA gain of function by sequestration of RNA-binding proteins to transcripts with expanded repeats, and 3) haploinsufficiency (Balendra). As a result, the neuropathology associated with C9orf72 mutation is complex, consisting of variable TDP-43 pathology as well as pathological features directly linked to the expanded repeats (Balendra). The association between this mutation and TDP-43 aggregation is also not known; however, none of the current mechanisms seem to be sufficient on their own, suggesting a more complex interplay between the different pathologies (Balendra).

2) TDP-43

TDP-43 is a highly-conserved, ubiquitously expressed 414 amino acid DNA/RNA-binding protein with a tightly autoregulated expression level (Wauters). This protein is mainly localized to the nucleus but has been shown to continuously shuttle between the nucleus and the cytoplasm (Wauters). TDP-43 is involved in multiple aspects of RNA metabolism in the nucleus and the cytoplasm, including transcription, splicing, mRNA transport and stabilization as well as stress granule formation,

binding to >6000 RNA species in the CNS with an enrichment for long transcripts and those related to neuronal development and synaptic functions (Rempe). Figure 1 shows the possible pathogenic

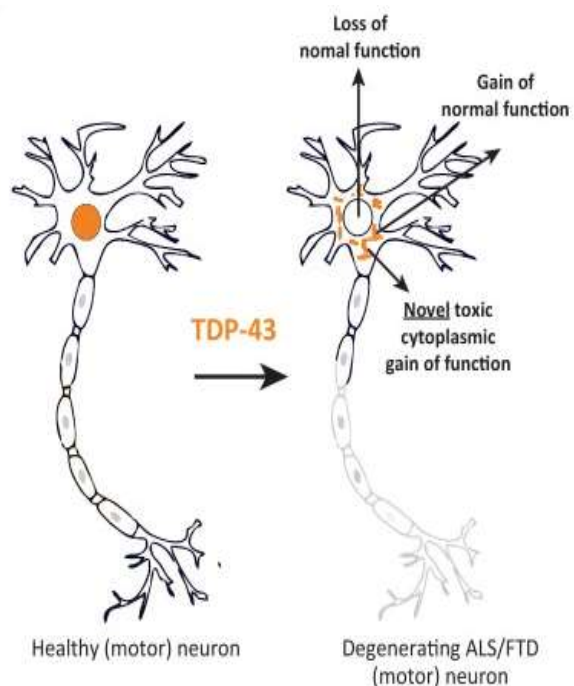


Figure 1: Loss of function vs. gain of function.

mechanisms of TDP-43 in FTD, including contributions of loss-of-function and toxic gain-of-function. The precise cell death mechanisms still remain to be determined; however, given the close association between nuclear TDP-43 depletion and cytoplasmic accumulation of post-translationally modified TDP-43 species, it is likely that complex disturbances of nuclear and cytoplasmic functions together with generation of toxic species may contribute to cell death (Roberson).

One of the major pathways suggested in FLTD-TDP is TDP-43's primary role in RNA metabolism, which becomes dysfunctional in FTD (Neumann). How cytoplasmic accumulation initiates remains a question, especially considering most cases are not caused by genetic mutation. Some have proposed a "multiple hit hypothesis" wherein the first hit is defective nuclear import, followed by cytoplasmic accumulation and aggregation of TDP-43 (Roberson). Other models implicate other key biological pathways in disease, including mitochondrial dysfunction, inflammation (particularly of microglia), RNA and protein transport, and the cytoskeleton (associated with FTLD-tau) (Roberson). There is increasing experimental evidence for prion-like propagation and progression as a common pathological mechanism in many neurodegenerative diseases (Roberson).

3) Mouse models of FTD

Mouse models have proven incredibly important for the study of human diseases including neurodegenerative disorders. Mice meet the need for an experimentally manipulative system that maintains sufficient genetic and neural conservation with humans including patterns of gene expression and structure across brain regions, particularly concerning FTD pathology associated proteins. Modelling FTD is challenging on many levels. FTD is a heterogeneous disorder with multiple phenotypic and pathological presentations and causative genetics -- for instance, multiple genetic mutations in FTD result in TDP-43 aggregation (Neumann). No one-to-one relationships occur despite some correlations having been identified between genetics, pathology, and clinical presentation.

Thus far, most studies modelling TDP-43 dysfunction have focused on ALS-associated motor phenotypes, as TDP-43 genetic mutations accounts for some familiar ALS cases, and from these models some options arise. Utilization of the CamKII promotor to produce dominant overexpression of TDP-43 mutants in the forebrain has been used to explore FTD-TDP mechanisms (Lisman). Transgenic CamKII-TDP-43 wildtype or mutant mice (lacking nuclear localization signal) present with significant early wide-ranging cognitive impairments and disrupted social interaction in addition to motor phenotypes (Lisman). Forebrain expression driven by CamKII promotor of even wildtype TDP-43 was sufficient to cause neurodegeneration and behavioural deficits (Lisman).

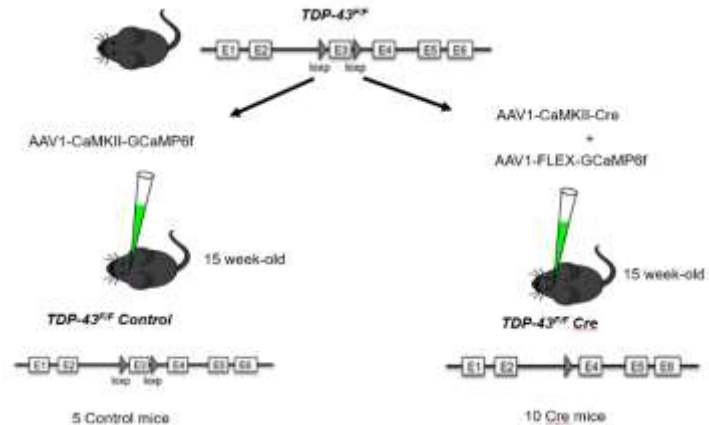
Complete TDP-43 knockout has proven lethal in mice both embryonically and rapidly upon post-natal induction. Heterozygous knockout allows mice to reach maturity but results in motor deficits in aged animals (Lisman). The Cre/LoxP system can be used to produce conditional loss of gene function in specific cell types such as neurons (M. Cecilia). This system also allows knockdown of the interested gene after developmental stage and during adulthood (M. Cecilia).

In this present study, we used the Cre/LoxP system to study the loss of function hypothesis, wherein TDP-43 was specifically knockout in the excitatory neurons of the prefrontal cortex. We hypothesize that TDP-43 nuclear depletion leads to neuronal loss in the prefrontal cortex. We aim to study the long-term consequence of TDP-43 clearance from the nucleus in the prefrontal cortex through histochemistry analysis.

Methods

Viral Injection and Sample Collection

Homozygous $TDP-43^{F/F}$ male mice were obtained from Dr. Philip Wong's group at Johns Hopkins University. A mix of viruses, AAV1-CamKII-Cre and AAV1-Flex-GCaMP6f, were bilaterally injected into the medial prefrontal cortex (mPFC) of 10 $TDP-43^{F/F}$ mice at the age of 3-4 months ($TDP-43^{F/F}$ Cre, Figure 2). This was done to selectively eliminate TDP-43 expression in the excitatory neurons of the mPFC and to simultaneously label these excitatory neurons with GCaMP6f, a green fluorescence calcium indicator. 5 $TDP-43^{F/F}$ mice were bilaterally injected with AAV1-CamKII-GCaMP6f to selectively label excitatory neurons at the mPFC with GCaMP6f. These mice



served as a control group ($TDP-43^{F/F}$ Control, Figure 2). A gradient-index (GRIN) lens was then implanted into one side of the prelimbic cortex of these above mice. Two months after the recovery from the implantation surgery, in vivo calcium imaging was performed once per month over a period of 6-10 months. After the completion of the longitudinal in vivo calcium imaging study, mice brains were collected. To collect mice brains, mice were perfused with phosphate buffer solution (PBS) followed by a fixation buffer containing 4% paraformaldehyde (PFA) in PBS. Fixed mice brains were then sectioned via a Vibratome (LEICA VT1200) and 60 μm coronal brain slices were collected for immunostaining.

Immunostaining

Sections were washed 3 times for 5 minutes each in PBS at room temperature with agitation then blocked for 2 hours in blocking solution consisting of 4% normal donkey serum, 1% BSA, and 0.3% triton-X-100 in PBS at room temperature with gentle agitation. Sections were then incubated with the primary antibody in 500 μL of blocking solution per section overnight at 4° C. Primary antibody for TDP-

43 is a rabbit polyclonal antibody (10782-2-AP, Proteintech) at 1:500 dilution. Primary antibody for NeuN is a mouse monoclonal antibody (ab104224, Abcam) at 1:1000 dilution. The next morning, sections were washed with PBS 5 times for 5 minutes each then incubated with the secondary antibody in blocking solution at room temperature for two hours with gentle agitation. Second antibody for TDP-43 is Alexa Fluor 594-conjugated Donkey-anti-rabbit-IgG at 1:400 dilution. Second antibody for NeuN is Cy5 conjugated Donkey-anti-mouse-IgG at 1:200 dilution. The plate containing the sections was wrapped in aluminum foil during the second incubation as the secondary antibody is light sensitive. Following the second incubation, the sections were rinsed 5 times for 5 minutes each with PBS at room temperature with agitation. The sections were then mounted. This was done by placing 1 drop of mounting medium containing DAPI on a microscope slide, mounting the brain section in the mounting medium (ensuring it was not folded), covering the section with a cover slip, and sealing the section with nail polish.

Confocal Imaging

The sections were imaged using a Zeiss 700 confocal laser scanning microscope with epifluorescence filters, Zeiss monochrome digital camera, and AxioVision ZEN software. DAPI was collected at SP 490, EGFP was collected at SP 555, and both Alexa594 and Cy5 were collected at LP 640 to minimize overlap of signals between filters. A 20x15 tile scan at 256x256 resolution was taken for each brain section to obtain a whole brain image. This whole brain image was then used to locate the medial prefrontal cortex (mPFC). A 12x10 tile scan image of the mPFC was taken with only DAPI to ensure the entire image was in focus; if it was not, two separate 6x10 images were taken, one of each hemisphere, with adjustments to the focus made as needed.

Following determination of focus, a 12x10 image was taken of the mPFC with only EGFP to determine location of the virus. The most intense EGFP signal was located then the signal intensity

adjusted to fall just below the intensity ceiling. Random locations throughout the mPFC were examined through Alexa594 and Cy5 filters to ensure signal intensities just below the intensity ceiling. A 12×10 image (or 2 6x10 images) was then taken with DAPI, TPMT, EGFP, Alexa594, and Cy5 filters at 1024x1024 resolution of the mPFC area.

Data Analysis

Images were then processed in ImageJ to obtain signal intensity data. Average signal intensities for brain regions with or without virus present as outlined in the figure below were taken as were three random background readings for all brain regions. Background was then subtracted out from the area average to obtain a true average signal intensity. The results were uploaded to Excel, then normalized. A Mann-Whitney U-Test was applied to test for statistical significance.

A ratio was obtained that describes the relationship between green, virus (+) TDP-43 and NeuN areas of the brain compared to non-green, virus (-) areas of the brain for TDP-43 and NeuN. This ratio indicates proportionally how many virus-infected cells show TDP-43/NeuN staining vs how many non-infected cells show TDP-43/NeuN staining. This ratio was obtained for both Control and Cre mice.

Results

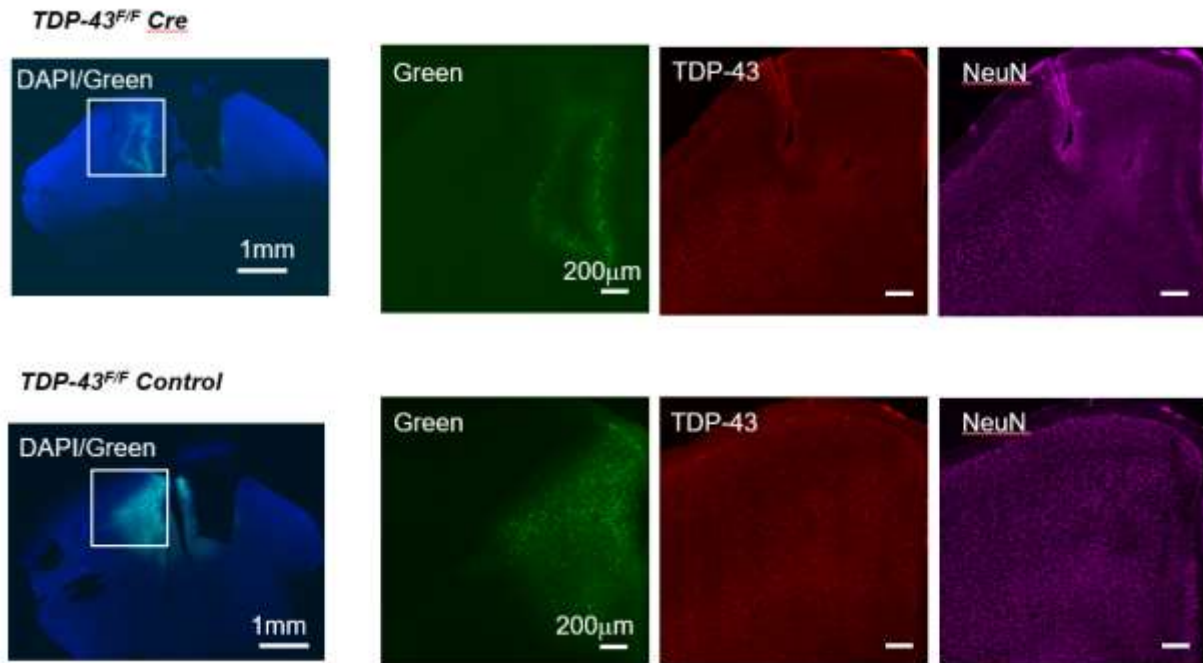


Figure 3: Representative Confocal images of control and Cre mice

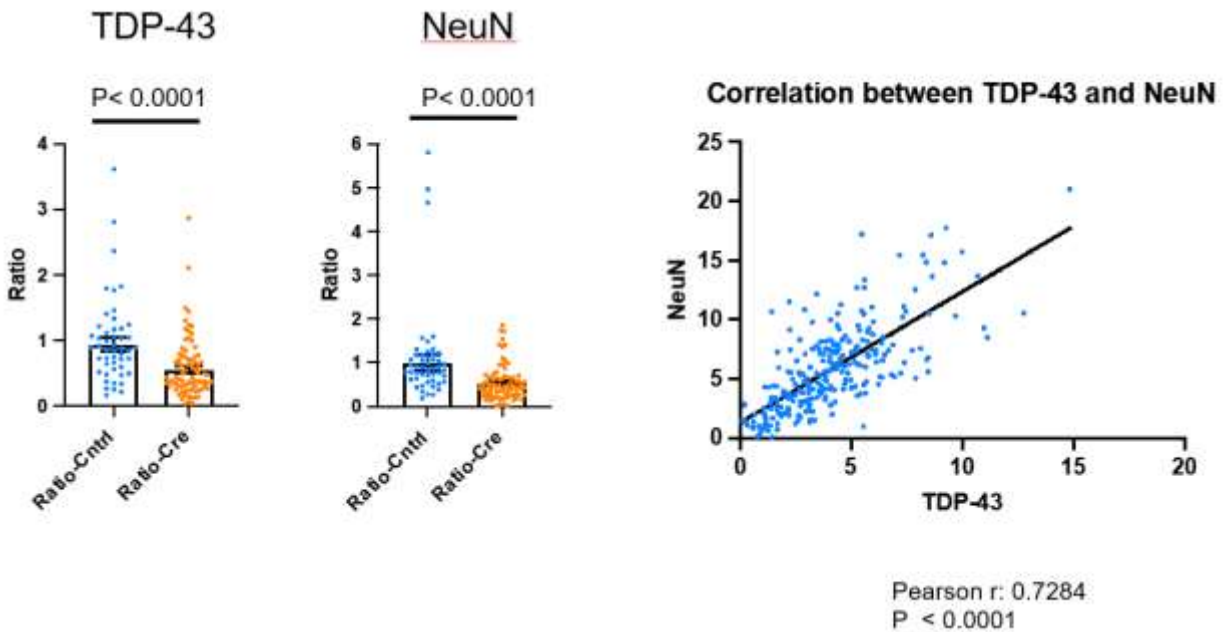


Figure 4: Statistical analysis results

Figure 3 shows the representative confocal images from the control and Cre mice in DAPI, EGFP, Alexa594, and Cy5 filters to show location of the virus, location of the TDP-43 protein, and location of nuclei of excitatory neurons (NeuN), respectively. Visually, the Cre mice show reduced signal intensity compared to the control mice across all three filters as indicated by dimmer or lack of signal in the mPFC.

Figure 4 shows the statistical analysis results of our study. Control mice show a ratio of approximately 1 for TDP-43 signal, whereas the Cre mice show a ratio of approximately 0.5 for TDP-43 signal. Similarly, Control mice show a ratio of about 1 for NeuN signal and Cre mice a ratio of about 0.5 for NeuN. Additionally, we see a strong positive correlation between TDP-43 signal and NeuN signal with a Pearson R of 0.7284. All findings have a p-value of < 0.0001 .

Ratios obtained for the TDP-43 staining match predicted values (Figure 4 left panel). For control mice, we would expect to see a ratio of approximately 1, indicating that TDP-43 expression in control viral-injected areas is about the same as that of non-viral-injected areas. For Cre mice, we would expect to see a reduced ratio for TDP-43 staining, indicating a successful elimination of TDP-43 expression in the presence of Cre recombinase at the Cre viral-injected area. We observed the ratio of approximately 0.55 in the Cre group, indicating that roughly 50% of neurons have TDP-43 nucleus depletion in the viral-injected area.

NeuN is a neuronal specific marker. Reduced NeuN typically suggests either neuronal loss or compromised neuronal function even if neurons still are present. Ratios obtained for the NeuN staining support our hypothesis that TDP-43 nucleus depletion leads to neuronal loss (Figure 4 middle panel). We observed ratio of approximately 1 in the control group, while a significant reduced ratio of NeuN staining in the Cre group. The ratio of approximately 0.53 in the Cre group, indicates roughly 50% of neurons were lost or compromised upon TDP-43 nucleus depletion in the viral-injected area.

There is also a positive correlation between TDP-43 signal and NeuN signal (Figure 4 right panel). NeuN stains the nuclei of live and functional neurons, and the TDP-43 signal indicates the presence of the TDP-43 protein. This positive correlation suggests that where there is a lack of TDP-43 protein, there is loss of neuron or functional compromised neuron.

Discussion

Our results support the loss of function FTD-TDP hypothesis. The ratios gathered through comparison of neural degeneration between areas with and without TDP-43 knockout suggest that TDP-43 knockout and neural death are positively related. Most likely, these neurons are dying, as the lack of NeuN signal indicates.

There is a possible alternate explanation for this owing to TDP-43's role in regulating RNA amount. As TDP-43 levels decrease, RNA levels will follow suit. Since NeuN is a nuclear protein, TDP-43 depletion might cause the decrease of NeuN RNA, this could make the NeuN expression too low to be detected by immunostaining. A possible solution for this that could be explored in future studies is the use of other types of stains, such as a Nissl stain or immunostaining with other apoptosis markers. Nissl stain is a nucleic acid staining method and therefore will stain nuclei and rough endoplasmic reticulum; while apoptosis markers can indicate if cells are dying. These could provide additional support for the loss of function hypothesis.

Overall, this project provides great insight into the mechanism behind neuronal death in FTD-TDP. Future research should continue this line of investigation in search of specific mechanisms underlying the loss of function hypothesis.

On a professional level, this project was a wonderful opportunity to work in an academic research lab, engage with experts in the field, and learn more about neuroscience research as it is actually conducted. I have learned a lot about how to construct and carry out neuroscience research and learned a wealth of new techniques that will be useful as I continue my education. Most importantly, I got to have this experience with a great team of wonderful, intelligent people who have set a high standard for me for work ethic and teamwork in the future. This experience has been invaluable and I am grateful for the opportunity to be part of this project. I will carry the lessons I have learned here with me and am grateful to the Honors College for giving me the opportunity to pursue this project.

Works Cited

- Balendra, R., & Isaacs, A. M. (2018). C9orf72-mediated ALS and FTD: multiple pathways to disease. *Nature reviews. Neurology*, 14(9), 544–558. <https://doi.org/10.1038/s41582-018-0047-2>
- Lisman, J., Schulman, H. & Cline, H. The molecular basis of CaMKII function in synaptic and behavioural memory. *Nat Rev Neurosci* 3, 175–190 (2002). <https://doi.org/10.1038/nrn753>
- M. Cecilia Ljungberg, Yousuf O. Ali, Jie Zhu, Chia-Shan Wu, Kazuhiro Oka, R. Grace Zhai, Hui-Chen Lu, CREB-activity and *nmnat2* transcription are down-regulated prior to neurodegeneration, while NMNAT2 over-expression is neuroprotective, in a mouse model of human tauopathy, *Human Molecular Genetics*, Volume 21, Issue 2, 15 January 2012, Pages 251–267, <https://doi.org/10.1093/hmg/ddr492>
- Neumann, M., & Mackenzie, I. R. A. (2019). Review: Neuropathology of non-tau frontotemporal lobar degeneration. *Neuropathology & Applied Neurobiology*, 45(1), 19–40. <https://doi.org/10.1111/nan.12526>
- Rempe, D., Vangeison, G., Hamilton, J., Li, Y., Jepson, M. and Federoff, H. (2006), Synapsin I Cre transgene expression in male mice produces germline recombination in progeny. *Genesis*, 44: 44-49. <https://doi.org/10.1002/gene.20183>
- Roberson, E.D. (2012), Mouse models of frontotemporal dementia. *Ann Neurol.*, 72: 837-849. <https://doi.org/10.1002/ana.23722>
- Solomon, D. A., Mitchell, J. C., Salcher, K. M. -T., Vance, C. A., & Mizielska, S. (2019). Review: Modelling the pathology and behaviour of frontotemporal dementia. *Neuropathology & Applied Neurobiology*, 45(1), 58–80. <https://doi.org/10.1111/nan.12536>
- Wauters, E., Slegers, K., Cruts, M., Van Broeckhoven, C., Chapter 8 - Frontotemporal dementia, Editor(s): Veerle Baekelandt, Evy Lobbstaël, Disease-Modifying Targets in Neurodegenerative Disorders, Academic Press, 2017, Pages 199-249, ISBN 9780128051207, <https://doi.org/10.1016/B978-0-12-805120-7.00009-9>.